Pergamon

Journal of Structural Geology, Vol. 17, No. 7, pp. 1035 to 1046, 1995
Copyright © 1995 Elsevier Science Ltd
Printed in Great Britain. All rights reserved
0191-8141/95 $9.50+0.00

0191-8141(94)00123-5

Present-day state of stress in northern Morocco from focal mechanism analysis

FIDA MEDINA

Université Mohammed V, Institut Scientifique, Département de Géologie, B.P. 703, Rabat-Agdal, Morocco

(*Received* 25 *November* 1993; *accepted in revised form* 27 *October* 1994)

Abstract—The use of focal mechanisms of micro-earthquakes and moderate teleseisms in the Al Hoceima area (northern Morocco) enables the determination of the state of stress in the southern part of the Gibraltar arc. Two different states of stress were determined: (1) a ENE–WSW extension in the Imzouren area (probably with similar magnitudes of σ_2 and σ_1) which may be controlled by pre-existing structures, and (2) a strike-slip regime in Beni Boucetta, Tamassint and Beni Abdallah areas (σ_1 NNW–SSE, σ_3 ENE–WSW in the two first areas and σ_1 NE–SW, σ_3 NW–SE in the latter). Contrary to recently proposed ideas, the mean state of stress determined with the help of moderate teleseisms corresponds to a strike-slip regime with a NNW–SSE oriented main compressional axis and a ENE–WSW horizontal extension, similar to the stress field determined from neotectonic studies, and somewhat different from that determined from the El Asnam aftershock sequence of 1980.

INTRODUCTION

The Gibraltar arc is the westernmost termination of the perimediterranean Alpine chains (Fig. 1). According to several authors (e.g. Andrieux *et al.* 1971, Leblanc & Olivier 1984, Philip 1987, Rebaï *et al.* 1992) the arc can be considered as the result of deformation of the small Alboran block between northwest Africa and Iberia since the early Tertiary. As a consequence of the NNW–SSE convergence between Africa and Iberia this block, delimited to the north by the Cadiz–Alicante fault (ENE–WSW) and to the southeast by the Nekor strike-slip fault (NE–SW) is being expulsed to the west-southwest where it overthrusts the foreland of the western Rif (Rebaï *et al.* 1992). This tectonic activity continues at present and is reflected by relatively important seismicity (Fig. 2). Earthquakes, concentrated along the Azores–Gibraltar fracture zone, become more diffuse and moderate ($M \leq 5$) east of the arc (Udias *et al.* 1976, Hatzfeld 1978, Cherkaoui 1988).

In the absence of *in situ* stress measurements and reliable microtectonic data from Quaternary formations, understanding of the present-day geodynamics and state of stress can only be inferred from regional seismicity and focal mechanisms of teleseisms (Udias *et al.* 1976, Hatzfeld 1978, Moreira 1985, Buforn *et al.* 1988, Buforn & Udias 1991, Medina & Cherkaoui 1992). However, low magnitude of these earthquakes, which are rarely followed by important aftershock sequences, and the poorly-adapted configuration of the regional

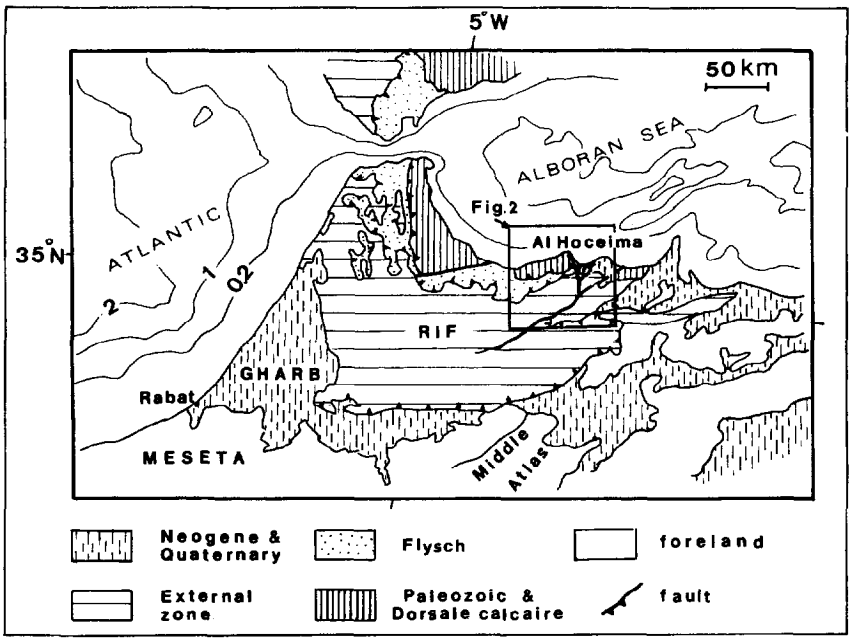

Fig. 1. Geological map of northern Morocco (from the tectonic map of Africa, 1/5 000 000, UNESCO). Sea depth in kilometres.

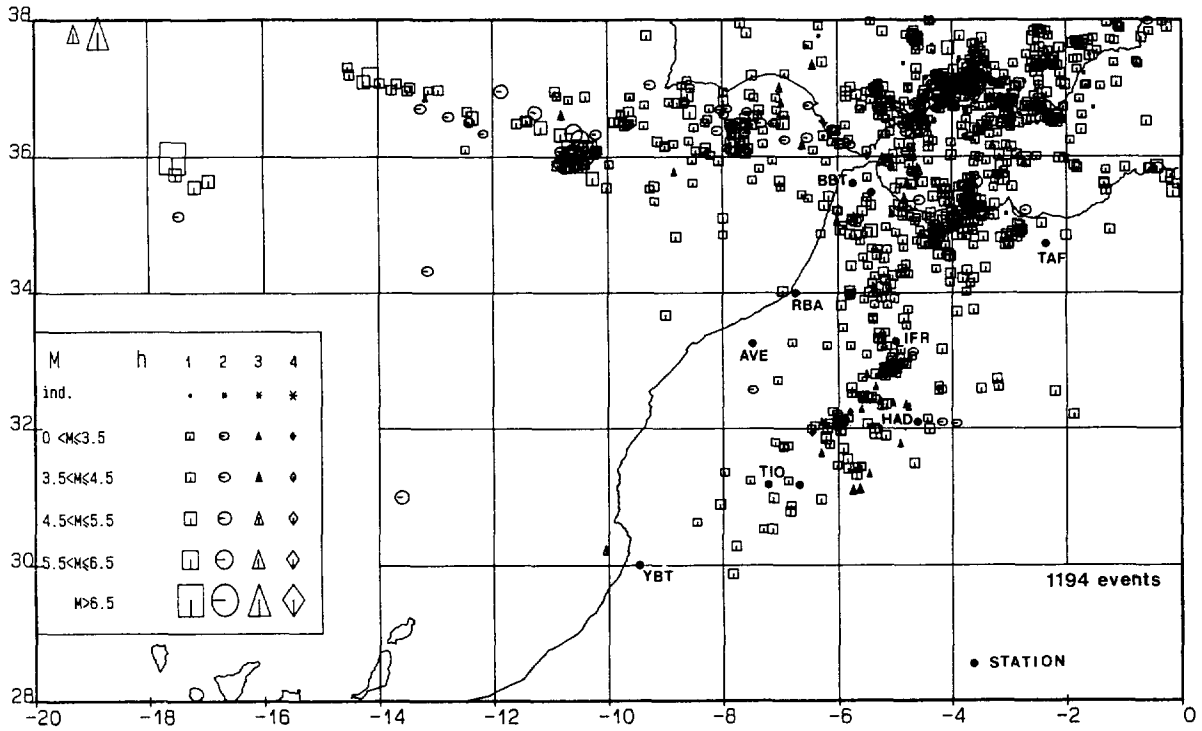

Fig. 2. Seismicity of Morocco (1923–1986) after Medina & Cherkaoui (1992). Only the events recorded by at least five stations, with horizontal and vertical errors less than 20 km, and with a RMS ≤ 2 s are represented. The numbers correspond to the following focal depths: (1) $0 < h \leq 35$ km; (2) $35 < h \leq 70$ km; (3) $70 < h \leq 150$ km; (4) $h > 150$ km. BBT, TAF, RBA, AVE, IFR, HAD, TIO and YBT are the seismological stations of the Institut Scientifique.

seismic networks generally leads to unreliable solutions. Some published results on the stress field are based on the assumption that the focal mechanism solutions reflect the state of stress, as the *P*-axis is considered to represent the main compressional stress σ_1 (Udias & Buforn 1991). Others have determined the stress with the right dihedra method by grouping a certain number of focal mechanisms covering a large area (Galindo-Zaldivar *et al.* in press). However, these mechanisms may not necessarily correspond to the same state of stress, as will be shown here. This paper is an attempt to reach a more accurate determination of the state of stress in the Al Hoceima area by applying the right dihedra method (Angelier & Mechler 1977), based on well-constrained data collected during a one-month micro-earthquake survey conducted in 1989 around the city of Al Hoceima (Fig. 3). The use of 16 portable stations facilitated the recording of an exceptionally large number of micro-earthquakes (Cherkaoui *et al.* 1990, Cherkaoui 1991), and consequently, the determination of a large set of reliable mechanisms. Of these, 41 were previously published in Hatzfeld *et al.* (1993). The purpose of the present paper is to study the state of stress and to compare the results with the available neotectonic and seismotectonic data.

GEOLOGICAL SETTING

Structural domains

The area of Al Hoceima is a part of the complex Rif chain, which runs along the northern coast of Morocco forming the southern branch of the Betic–Rif arc (Fig. 1). Near the city, the most important structural domains are (Fig. 3):

(1) The Bokkoya, a calcareous unit consisting of tectonically-complex nappes of Palaeozoic elements and their thick Triassic and Jurassic and thin Cretaceous to Eocene cover. This unit formerly belonged to the margin of the Alboran block (Andrieux 1971, Mourier 1982, Leblanc & Olivier 1984);

(2) The Tiziren unit, comprising Middle Jurassic–Early Cretaceous carbonates and radiolarites (1000 m) overlain by a thick (2000 m) Valanginian to Barremian flysch series. This unit is separated from the Bokkoya by a narrow east–west zone: the 'semelle triasique' (Andrieux 1971) composed of Oligocene conglomerates, marls, sandstones and limestones;

(3) The Ketama metamorphic unit, which consists in the studied area of an Early Cretaceous flysch series and Cenomanian–Turonian limestones and calcareous slates. Towards the northeast, this unit is overlain by the Ras–Tarf andesites, which yielded middle Miocene ages (12.2–15.7 Ma; Guillemin & Houzay 1982, p. 127). To the south, the Ketama unit is separated from the Temsamane unit by the Nekor fault;

(4) The lower Nekor basin, a triangular graben located southeast of Al Hoceima, which runs north–south cross-cutting the previous units. Drillholes for water prospection show that up to 400 m of Quaternary alluvial deposits overlie a thin series of marls (Messinian?) and the Ketama unit (Thauvin 1971, p. 74). Recent Quaternary tectonic activity is attested by differences in thickness of the alluvial deposits, reaching 40 m between neighbouring drillholes;

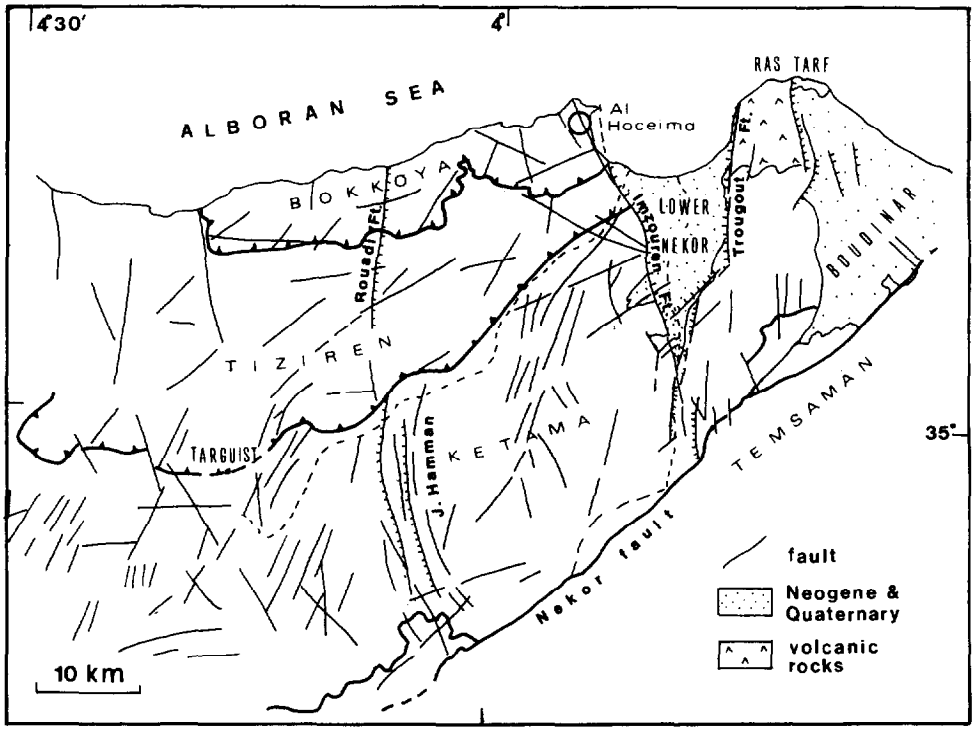

Fig. 3. Structural domains and fault pattern in Al Hoceima area, after Maurer (1968), Andrieux (1971), Suter (1980) Guillemin & Houzay (1982) and Frizon de Lamotte (1982) and completed by the interpretation of Landsat-MSS imagery.

(5) The Boudinar basin east of Ras–Tarf Cape, consisting of Miocene and Pliocene marls and conglomerates.

Major faults

Figure 3 shows the main faults in the area, based on mapping by Maurer (1968), Andrieux (1971), Suter (1980), Guillemin & Houzay (1982) and Frizon de Lamotte (1982). Lineaments (only those interpreted as possible faults are represented) observed from Landsat-MSS imagery have been added to the map, in order to compare the superficial faults to the distribution of the epicentres and to try to determine the main faults from the focal mechanisms. The map shows that, in addition to the east–west to northeast–southwest thrust and vertical faults which delimit the different structural domains, there are several other almost-vertical faults, trending mainly north-northwest–south-southwest. The most important faults are:

(1) the Imzouren fault (NNW–SSE), which delimits the western boundary of the lower Nekor basin. This fault, which is not drawn on the current geological maps, was interpreted by Thauvin (1971) and confirmed by Morel (1992) and by the observation of space imagery. The length of the trace is about 21 km;

(2) the Trougout fault, trending roughly north–south, which runs along the eastern boundary of the lower Nekor basin (15 km), and which extends another 15 km southwards after a shift of 5 km to the west;

(3) the Jbel Hammam fault system (NNW–SSE), consisting of several normal faults with trace lengths of 20 km. The western block is the downthrown one;

(4) the Rouadi fault, trending NNE–SSW over 15 km, thought to be the northern continuation of the Jbel Hammam fault system. However, the eastern block is downthrown here (Maurer 1968, Morel 1987).

Other, apparently small, faults are visible in Fig. 3, e.g. those within the Ketama unit east of Jbel Hammam and southeast of Targuist. The displacement along the fault planes is not well determined because of the absence of recent formations, but cartographically they display strike separation.

Recent tectonic history

Most authors agree that, after the pre-Messinian emplacement of the Rif nappes, normal and strike-slip motion along the faults was predominant. Structural analysis carried out by Frizon de Lamotte (1982, p. 297) Chotin & Aït Brahim (1988) and Galindo-Zaldivar *et al.* (in press) shows that a horizontal σ_1 underwent a counterclockwise rotation: east-northeast–west-southwest during the Tortonian, north-northeast–south-southwest during the end-Tortonian, and northwest–southeast in the Plio-Quaternary, even though a more complex evolution involving extensional episodes is inferred from local studies (Groupe de Recherche Néotectonique de l'Arc de Gibraltar 1977). The fault activity related to the state of stress is discussed below.

PREVIOUS WORK ON SEISMICITY AND SEISMOTECTONICS

The seismicity around Al Hoceima was studied by several authors because of the frequency of events and the presence of the Nekor fault which represents the

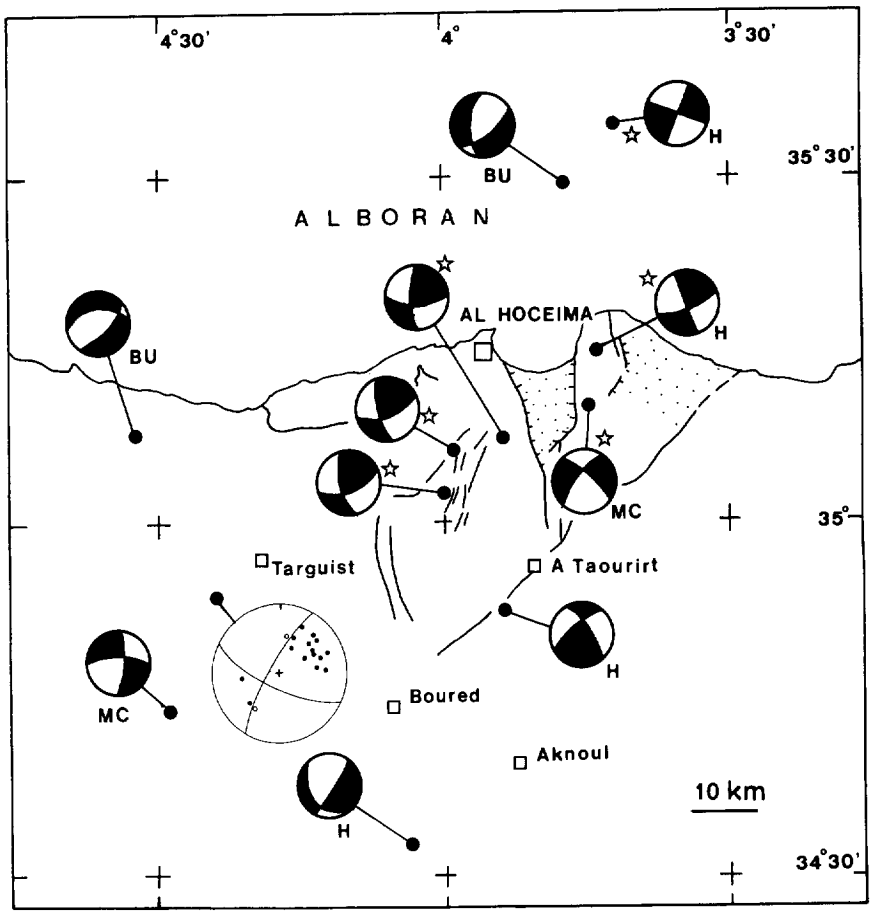

Fig. 4. Focal mechanisms of moderate teleseisms in the Central Rif area. H, after Hatzfeld (1978); MC, after Medina & Cherkaoui (1992); BU, after Buforn & Udias (1991). Those marked with a star have been used to determine the mean stress field. The solution with indicated first motions (near Targuist) is composite and based on data from Hatzfeld *et al.* (1977).

major structural element in northern Morocco. Such studies concern seismicity and seismotectonics (Hatzfeld *et al.* 1977, Frogneux 1980, Aït Brahim *et al.* 1990, Cherkaoui *et al.* 1990, Buforn & Udias 1991, Medina & Cherkaoui 1992, Asebriy *et al.* 1993, Hatzfeld *et al.* 1993) as well as seismic hazards (Bentaleb *et al.* 1984, Cherkaoui 1991). The main conclusion is that seismicity is most important north of the Nekor fault and decreases notably to the south. The depth of the foci is generally shallow. From the regional seismicity maps, it appears that there is no clear correlation between geological structures and the distribution of epicentres, although some authors, e.g. Aït Brahim *et al.* (1990) state that such a correlation exists. However, the horizontal error on the epicentre location (20–30 km according to Cherkaoui 1988) is too large for trying to define active faults comparable, for instance, to the San Andreas system along which the epicentres display a more or less linear pattern. The focal mechanisms of the most important teleseisms (Fig. 4) show different solutions, but all have a strike-slip component, with the P and T axes interchanging. However, a more detailed look into the data set on which some of these mechanisms are based leads to the conclusion that their reliability is far from being perfect because of contradictory arrivals of P-waves and of uncertainties in depth and take-off angles (see discussion in Medina & Cherkaoui 1992).

DISTRIBUTION OF MICRO-EARTHQUAKES

Three hundred and sixteen micro-earthquakes were recorded during the survey of October/November 1989 (Fig. 5). However, as the orientation and dip of the fault planes of the focal mechanism solutions depend strongly on the accuracy of the locations, the events retained are those with small vertical and horizontal errors (less than 2 km), low residuals ($\leq$0.2 s) and a number of phases equal or exceeding 10. Detailed description of the methodology of selection is described by Cherkaoui *et al.* (1990), Cherkaoui (1991) and Hatzfeld *et al.* (1993). These constraints leave 231 events, most of which belong to four clusters (Fig. 5).

The first cluster, located near Imzouren forms a more or less linear zone oriented NNW–SSE, running along the northwestern boundary of the lower Nekor plain, and containing 42.9% of the recorded events. The second cluster is located immediately south of the first (Beni Boucetta), and consists of 77 events, which form a 15 km-long and 8.5 km-wide strip running north–south. The third group is represented by a cluster of 14 epicentres located at 35°06′N–3°54′W, near Tamassint. The fourth and last group is located southeast of Targuist. The epicentres form a strip 26.5 km-long and 8.5 km-wide.

Two hundred and thirty-six events have focal depths

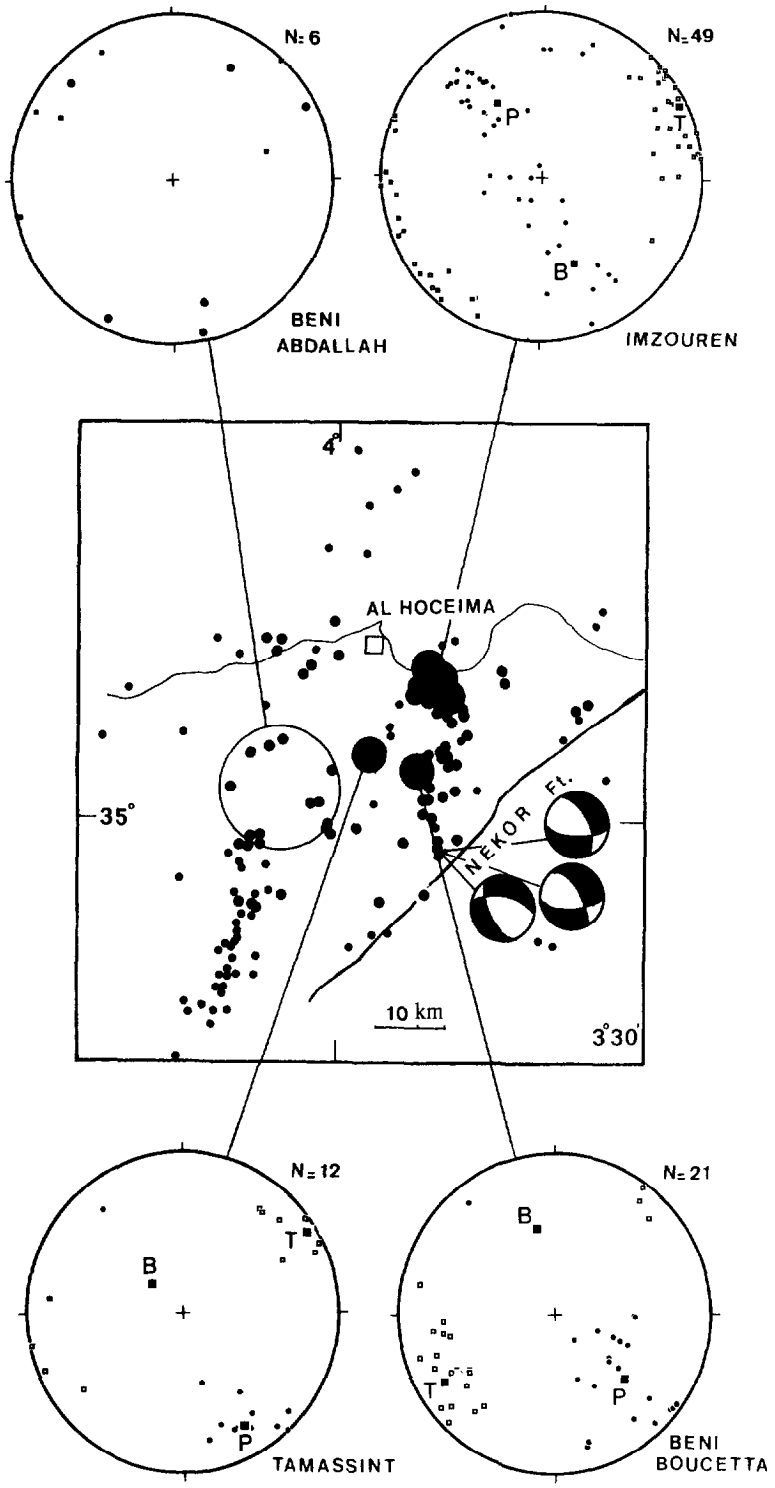

Fig. 5. Microseismicity in the Al Hoceima area during the period of 17 October to 17 November 1989 (after Cherkaoui *et al.* 1990). Large dots—important seismic sources; medium-size dots—well-constrained epicentres (ERH and ERZ ≤ 2 km, RMS ≤ 0.2 s); small dots—poorly-constrained epicentres. Distribution of *P* (dots) and *T* (squares) axes of focal mechanisms of earthquakes is shown in stereograms (Schmidt net).

between 4 and 12 km, and the vertical sections show that the clusters near Imzouren and Targuist may reflect almost-vertical fault planes (Cherkaoui *et al.* 1990), although application of the constraints on the location of the foci does not leave more than a few epicentres in the latter area.

FOCAL MECHANISMS

The large number of collected data allows the determination of 187 individual focal mechanisms. A selection was made in order to exclude those with doubtful first motions or with poorly-constrained nodal planes.

Table 1. Eigenvalues and trend of vectors of the kinematic axes

Kinematic axes	Eigenvalues	Trend	Plunge
Imzouren (N = 49)			
1	0.2759	327.1	46.7
2	0.1099	157.9	42.8
3	−0.3858	62.9	5.4
Beni Boucetta (N = 21)			
1	0.3701	132.1	38.9
2	0.0347	348.7	44.9
3	−0.4048	238.4	19.2
Tamassint (N = 12)			
1	0.4227	150.8	20.3
2	0.0037	312.0	68.7
3	−0.4263	58.4	6.3
Beni Abdellah (N = 3)			
1	0.4036	39.8	8.5
2	0.0173	159.2	73.0
3	−0.4209	307.6	14.6
Teleseisms (N = 6)			
1	0.3360	318.8	0.4
2	0.0340	227.8	66.4
3	−0.3700	49.0	23.6

Eighty-eight events were finally retained, some of which were taken from the 41 mechanisms already published by Hatzfeld *et al.* (1993). The different types of mechanisms are reviewed below in some detail. The orientation and eigenvalues of the mean P and T axes were determined with Bingham distribution statistics (Marrett & Allmendinger 1990) using the computer program Fault Kinematics 2.1 (Allmendinger *et al.* 1989) (Fig. 5 and Table 1). Theoretically, these axes do not necessarily reflect the stress and strain axes, especially for shallow earthquakes (McKenzie 1969), but they correspond to infinitesimal strain axes (Marrett & Allmendinger 1990).

The focal mechanisms of the events belonging to the cluster located near Imzouren show solutions with either normal motion, or strike-slip faulting with a normal component (Figs. 5 and 6). The T axes are east-northeast–west-southwest, the P axes being either almost-vertical for the normal solutions or northwest–southeast for those showing strike-slip motion. The mean P and B axes trend northwest–southeast and are clearly oblique, plunging respectively towards the north-northwest and the south-southeast. The mean T-axis is horizontal and oriented east-northeast–west-southwest (Fig. 5). The main fault plane is probably oriented north-northwest–south-southeast since the cluster shows this trend and appears to be related to the Imzouren fault. The displacement is then either sinistral with a normal component, or purely normal.

In Beni Boucetta, the micro-earthquakes are mainly aftershocks of an event recorded on 7 November 1989. Most solutions show a gently NE-dipping plane or a N–S-trending plane (Hatzfeld *et al.* 1993), dipping either steeply to the west (normal solutions) or steeply to the east (reverse solutions). The T axes trend ENE–WSW, and most P axes have a SSE-plunge. The mean P and B axes have a NNW–SSE trend, and are also oblique (Fig. 5). The fault planes are probably those oriented N–S according to the geological maps (Fig. 3) and to the epicentre distribution (Fig. 5). The motion is then either purely normal, or normal with a left-lateral component. On a triangular diagram, most mechanisms fall in the zone of 'odd' earthquakes (Fig. 6), contrary to the Imzouren cluster. Further south, three focal mechanisms show mostly normal faulting. One solution is similar to those of the Beni Boucetta area, with N–S-trending planes, and two other solutions also correspond to normal faulting, but with a T axis oriented NE–SW.

The best-constrained solutions obtained in the area of Tamassint mainly belong to two groups. The first (10 events) shows strike-slip faulting with a normal component, while the second (2 events) shows also strike-slip faulting, but with a reverse component. The P axes plunge slightly towards the south-southeast in most solutions (Fig. 5). The mean P axis is horizontal, B is oblique and T is horizontal with a ENE–WSW trend. On a triangular diagram (Fig. 6), most mechanisms fall within the strike-slip sector. As the predominant fault trends are north-northeast–south-southwest on the geological maps, the planes with this trend are interpreted as the main fault planes. The motion is then sinistral strike slip, with slight variations in the plunge of the slip vector.

Near Beni Abdallah, the mechanisms are quite different from those in other zones. Here, two sets of solutions are obtained: three events show strike-slip faulting with a normal or reverse component. The P axes plunge towards the southeast, and the T axes are northeast–southwest (Fig. 5). The planes are not well-constrained because of the absence of stations towards the southwest. Three other mechanisms correspond to strike-slip motion but with P and T axes respectively northeast–southwest and northwest–southeast (Fig. 5). This is completely different from the other solutions and needs further explanation (see below).

In the area southeast of Targuist and despite the number of earthquakes recorded, it was not possible to determine the focal mechanisms, as the epicentres are located outside the network. The P-wave first arrivals, mostly compressions, are similar to those obtained by Hatzfeld *et al.* (1977, p. 745), who did not propose a solution since the seismicity was thought to be related to the Nekor fault. A composite solution with strike-slip faulting is proposed here on the base of the same data, and taking into account the presence of a north-northeast–south-southwest alignment of epicentres (Fig. 5). The N 25°E fault, which we consider as the main fault, is then left-lateral. This solution has a well-constrained north-northeast–south-southwest plane whereas the other plane remains poorly defined. This interpretation, however, is very different from that of Aït Brahim *et al.* (1990) who proposed on the basis of regional seismicity maps (with no constraints on epicentre location) that the sysmogenic zone of Targuist reflects the deep and active continuation of the northwards gently-dipping thrusts of the Rif front located to the south.

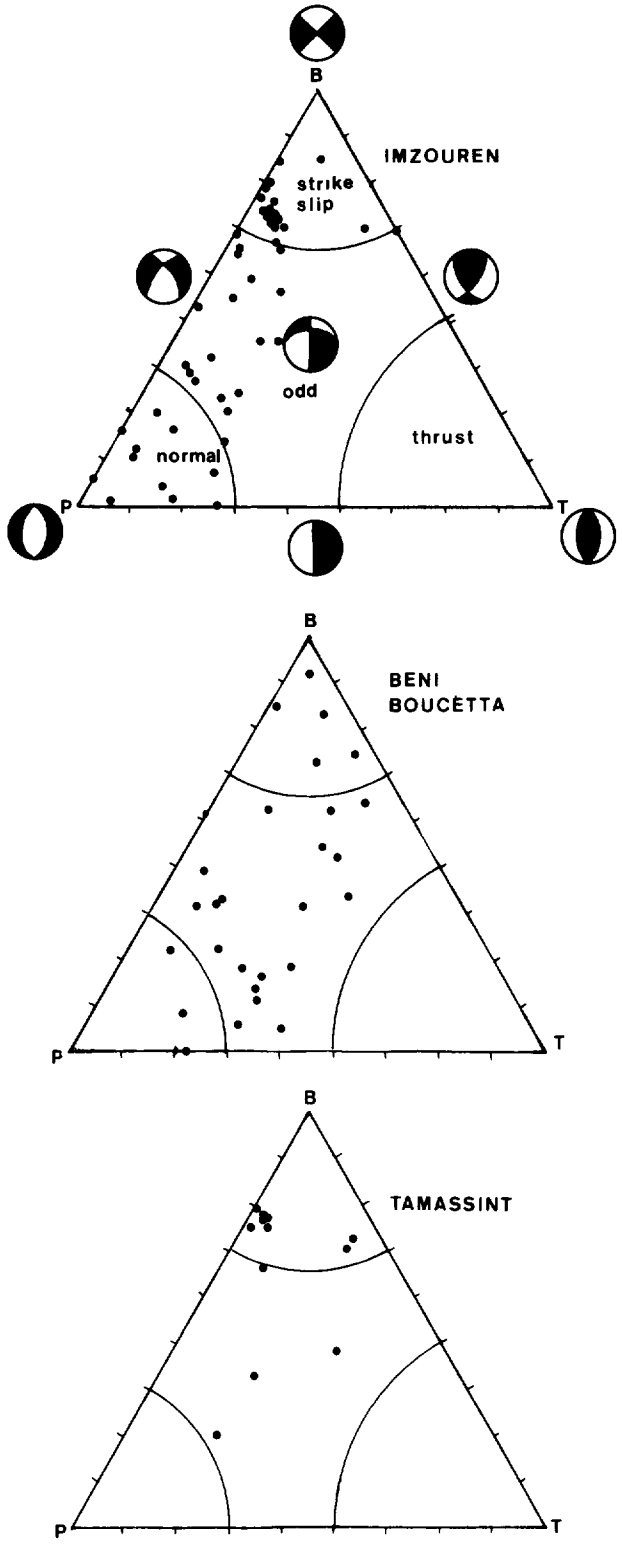

Fig. 6. Triangular diagrams (Frohlich & Apperson 1992) representing the plunge of *P*, *T* and *B* axes for the three clusters of Imzouren, Beni Boucetta and Tamassint.

STATE OF STRESS

The state of stress was determined with the dihedra method (Angelier & Mechler 1977). Although this method is somewhat imprecise in comparison with the numerical inversion methods (e.g. Carey & Brunier 1974, Carey 1979, Angelier & Goguel 1979, Etchecopar *et al.* 1981, Armijo *et al.* 1983), it has been chosen because it is simple, can be controlled manually, does not require a choice of fault planes, and is easily applied on micro-computers (Allmendinger *et al.* 1989). In addition, the dihedra method has been already successfully used for first-order determination of the state of stress from teleseisms and microseismicity (Carey-Gailhardis & Mercier 1987, 1992, Galindo-Zaldivar *et al.* in press). The detailed comparison of dynamic and kinematic methods applied for microtectonic and focal mechanism data (Angelier 1975, Marrett & Allmendinger 1990)

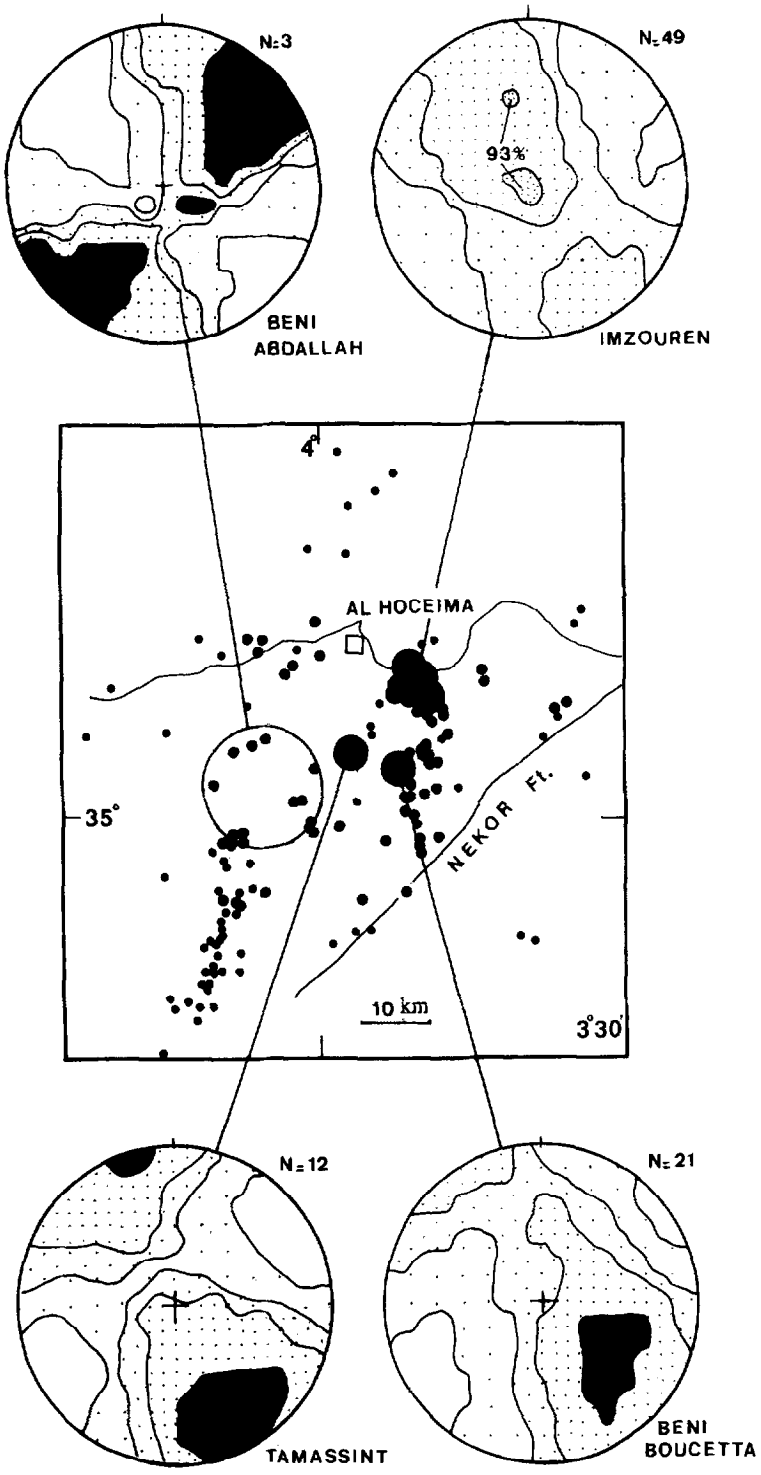

Fig. 7. State of stress in the Al Hoceima area determined from micro-earthquakes, with the dihedra method (Schmidt net). Black sectors: 100% compression; white sectors 0% compression (100% extension); intermediate sectors: 1–33%; 34–66% and 67–99% compression.

leads to the conclusion that both methods give comparable results for the purposes of this study.

The 49 most reliable solutions obtained for the Imzouren cluster show both normal and strike-slip motions. Plotting the axes P, T and B of each event on a triangular diagram (Frohlich & Apperson 1992) reveals that most events fall between strike-slip and normal mechanisms, but with a remarkable continuity, since there are no separated groups of pure strike-slip and pure normal faults (Fig. 6). Moreover, the plunge of the P and T axes is not influenced by depth (change of fault dip or different motions on closely spaced planes as in the case of the Aegean arc according to Hatzfeld *et al.* 1987) nor by timing of events. Therefore, a single diagram was constructed for all data. The P-dihedra contour shows a well-constrained ENE–WSW-trending extension and a less-constrained compressional stress sector (Fig. 7). The absence of a 100% compressional (49 events) sector is interpreted to be due to the proximity of values of σ_1 and σ_2, but not to the existence of

Table 2. List of teleseisms and focal mechanism parameters used for the determination of the mean stress field (only P and T are given)

Date	Lat (°N) Long (°W)	Mag.	h (km)	P tr.(°)	P pl.(°)	T tr.(°)	T pl.(°)
17 April 1968	35°14′ × 3°43′	5.0	13	305	10	036	06
14 July 1974	35°34′ × 3°42′	4.3	2	170	00	260	00
15 July 1977	35°10′ × 3°44′	3.7	17	170	32	262	03
21 April 1979	35°02′ × 4°00′	3.8	5	300	07	035	36
20 March 1981	35°08′ × 3°54′	3.9	5	294	17	034	23
7 April 1981	35°07′ × 3°59′	3.7	5	310	10	047	33

incompatible fault motions. This is confirmed by the lengthened shape of the contours, which may reflect a ratio R close to 0.75.

For the Beni Boucetta cluster, the dihedra contour shows that σ_1 is oblique, plunging towards the southeast whereas σ_3 is nearly horizontal. Anyway, σ_1 is not poorly defined as in the previous example.

The dihedra contour of the Tamassint cluster shows well-defined compressional sectors, with σ_1 oriented NNW–SSE and σ_2 NE–SW (Fig. 7). This pattern is not very different from that obtained from the Beni Boucetta cluster, because the compressional sectors overlap slightly.

In Beni Abdallah three mechanisms differ considerably from the others since the main compressional and extensional axes have respectively northeast–southwest and northwest–southeast trends (Fig. 7). These mechanisms have not been included in a previous study (Hatzfeld *et al.* 1993) because the coverage of the focal sphere was less than 75%. However, they are considered as interesting since they reflect local reorientations of the stress axes. Because of the incompatibility of the fault motions, the diagram in Fig. 7 is constructed for the mechanisms with northeast–southwest P-axes.

INTERPRETATION AND DISCUSSION

Stress field in the northern Rif area

The data presented here indicate that the state of stress is extensional in the Imzouren area and strike-slip near Beni Boucetta and Tamassint. It seems that, when moving from the lower Nekor graben to the southwest, σ_3 remains horizontal along the ENE–WSW trend, whereas σ_1, vertical (and poorly defined) at Imzouren, changes to horizontal in the west.

On a larger scale, several investigators have tried to determine the state of stress in the Gibraltar area from focal mechanisms, either by considering that the P axis is equivalent to σ_1 (Udias & Buforn 1991), or applying the dihedra method to focal mechanisms of teleseisms (Galindo-Zaldivar *et al.* in press). It is commonly uncertain if the P axis is coaxial with σ_1 since the latter can be located anywhere in the compressional dihedron if the rock volume is previously fractured or affected by some internal discontinuities, as it is generally the case (McKenzie 1969). Galindo-Zaldivar *et al.* (in press) found an inconsistency between the only focal mechanism they used in the Rif (taken from Buforn & Udias 1991, see mechanism BU in Fig. 4), which shows NW–SE extension, and the general trend of the regional compressional stress axis (NNW–SSE). They conclude that the state of stress in the Rif is different from that determined in the surrounding areas. It is shown here that this inconsistency is only due to the fact that the focal mechanism used is very poorly-constrained (contradictory P-wave arrivals to the Spanish stations, and no more than three data points from the south). Therefore, it appears that there is no drastic reorientation of the stress field which appears to be similar to that determined in the surrounding areas, as inferred from neotectonic and plate kinematic data, which predict a NNW (N 140° to N 160°E) shortening, in relation to a pole located close to the Canary Islands (Minster & Jordan 1978, Argus *et al.* 1989).

Mean or local state of stress

This study raises the question whether the state of stress determined from the micro-earthquakes (of magnitude 1 to 3) really reflects the mean state of stress in the eastern Rif area, or local block adjustments only. This problem has recently been studied by Carey-Gailhardis & Mercier (1992) who concluded that, contrary to large earthquakes ($M \geq 6$), micro-earthquakes do not necessarily reflect the mean state of stress, and that some seismic fault motions may be due to internal deformations of blocks. The state of stress can then be modelled by different stress deviators which remain, however, coaxial with the mean. A similar problem was also studied by Hippolyte *et al.* (1992) from neotectonic data collected in southern Italy, where they observed frequent permutations of the stress axes, particularly between σ_1 and σ_2.

In order to compare the states of stress obtained from microseismicity to that inferred to be the mean state of stress, mechanisms of six moderate earthquakes were used to determine the latter. Two mechanisms were taken from Hatzfeld (1978) and Frogneux (1980), one from Medina & Cherkaoui (1992) and three are still unpublished (Table 2). The other mechanisms were not taken into account, as they are either far from the studied area, or rely on doubtful data. The mechanisms presented are the most reliable and correspond to shallow shocks located in a narrow region between 35°02′N; 35°34′N; 3°42′W and 4°03′W. All the solutions are strike-slip, with horizontal P and T axes oriented re-

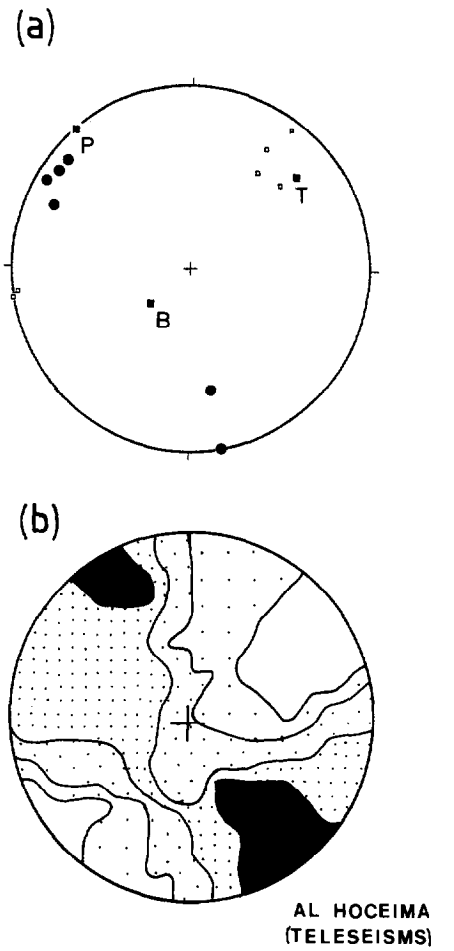

Fig. 8. (a) Distribution of P, T and kinematic axes (Schmidt net). (b) State of stress from teleseisms. Symbols as in Fig. 7.

spectively NNW–SSE to N–S and ENE–WSW to E–W (Figs. 4 and 8a). The dihedra diagram (Fig. 8b) suggests horizontal compressional and extensional axes, and is in good accordance with the diagram obtained from Tamassint and Beni Boucetta. If we admit this to be the mean regional state of stress, then the diagram of Imzouren may only reflect a local state of stress, with a permutation of σ_1 and σ_2. However, it is not certain that they correspond to internal block deformations since, if local geology is taken into account, the pre-existing north-northwest–south-southeast fault planes are parallel to the trend of the compressional stress; they may therefore act as normal faults in response to the stress direction. This assumption is supported by the structural pattern, since the lower Nekor basin appears cartographically as a triangular graben delimited by two normal faults at its edges. Therefore, the state of stress in the Imzouren area seems to be controlled by the pre-existing structures.

Permutation of stress axes

As indicated above, the dihedra diagrams suggest a spatial permutation of the main stress axes over the area. In the Imzouren, Beni Boucetta and Tamassint areas, σ_3 remains east-northeast–west-southwest, whereas σ_1, vertical at Imzouren, becomes oblique at Beni Boucetta and horizontal at Tamassint. This is a 'classical' σ_1/σ_2 permutation. Farther west, in Beni Abdallah area, there is another type of permutation involving σ_1 and σ_3, σ_1 becoming northeast–southwest and σ_3 northwest–southeast. This configuration confirms that observed in a focal mechanism of a large earthquake located southwest of Targuist (Fig. 4). In the opinion of the present author, the permutations may be explained by two factors: it could mean that the strain produced by the extension trending ENE–WSW is accommodated in the neighbouring areas to the west, or that the NNW–SSE compression produces expulsion of blocks towards the southwest in a similar manner to that suggested by Fraissinet (1989) and Zouine (1993) in the High Atlas chain. These authors observed two contemporaneous perpendicular stress directions. Thus, the NNW–SSE shortening is accompanied by local E–W compressions. Another explanation may be a 'corner effect' as that described by Rebaï *et al.* (1992) in southern France. In the case of the Rif chain, it is known that some of the structural units formerly belonged to the Alboran block (Andrieux *et al.* 1971, Leblanc & Olivier 1984). According to our data, this block seems to undergo expulsion, perhaps along the Nekor fault, as depicted in Fig. 9.

Finally, the presence of simultaneous different states of stress in such a small area brings up the question whether the separation of 'tectonic phases' in microtectonic studies is valid. It appears necessary, as also stated by Hippolyte *et al.* (1992) and Rebaï *et al.* (1992), to imagine that several states of stress may be contemporaneous and that the separation in 'tectonic phases' may sometimes be artificial.

CONCLUSIONS

The use of the focal mechanisms of microearthquakes and moderate teleseisms in the Al Hoceima area leads to the following conclusions:

(1) Two separate states of stress occur in the area.

(2) The mean state of stress corresponds to a strike-slip regime, with a NNW–SSE main compression and a ENE–WSW horizontal extension. This stress field is in continuity with that known in Quaternary times (Frizon de Lamotte 1982, Chotin & Aït Brahmin 1988). However, it is somewhat different from the state of stress deduced from the aftershock sequence of the El Asnam earthquake of 1980 (Ouyed 1981), which corresponds to a compression (σ_1 NNW, horizontal; σ_2 and σ_3 being either horizontal or vertical). It is also notable that no thrust mechanisms were recorded during the survey, as would be expected from the structure of the Rif.

Acknowledgements—This paper is the geologist's point of view of an extensive seismological program carried out in 1989 with my colleagues T.-E. Cherkaoui and H. Jebli from the Département de Physique du Globe of the Institut Scientifique at Rabat and D. Hatzfeld and V. Caillot from the Université Joseph Fourier at Grenoble, with the support of the Action Intégrée 359/88. I would like

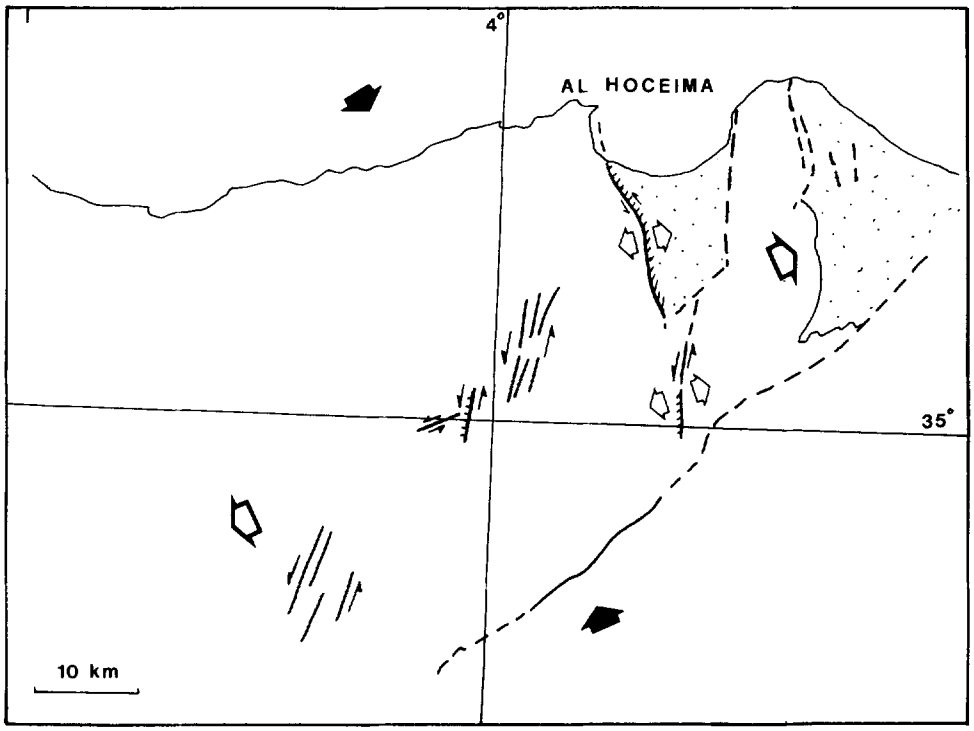

Fig. 9. Active faults and their motion in the area of Al Hoceima during the micro-earthquake survey of October/November 1989.

to dedicate it to the memory of Dr Hassan Jebli (born 1949) who died unexpectedly at Grenoble, 1 April 1994. The paper has benefitted from the critical and constructive comments of R. Allmendinger and J.-L. Mercier, A. Charroud provided the Fault Kinematics Program.

REFERENCES

Aït Brahim, L., Chotin, P., Tadili, B. & Ramdani, M. 1990. Failles actives dans le Rif central et oriental. *C. r. Acad. Sci. Paris, sér II*, **310**, 1123–1129.

Allmendinger, R. W., Marrett, R. A. & Cladouhos, T. 1989. Fault Kinematics version 2.0, a program for analyzing fault slip data. (Unpublished document.)

Andrieux, J. 1971. La structure du Rif central. Etude des relations entre la tectonique en compression et les nappes de glissement dans un tronçon de la chaîne alpine. *Notes & Mém. Serv. géol. Maroc.* **235**.

Andrieux, J., Fontboté, J. M. & Durand-Delga, M. 1971. Sur un modèle explicatif de l'Arc de Gibraltar. *Earth Planet. Sci. Lett.* **12**, 191–198.

Angelier, J. 1975. Sur l'analyse des mesures recueillies dans les sites faillés: l'utilité d'une confrontation entre les méthodes dynamiques et cinématiques. *C. r. Acad. Sci. Paris, sér D*, **281**, 1805–1808.

Angelier, J. 1983. Analyses qualitative et quantitative des populations de jeux de failles. *Bull. Soc. géol. Fr.* XXV, **5**, 661–672.

Angelier, J. & Goguel, J. 1979. Sur une méthode simple de détermination des axes principaux des contraintes pour une population de failles. *C. r. Acad. Sci. Paris, Sér. D*, **288**, 307–310.

Angelier, J. & Mechler, P. 1977. Sur une méthode graphique de recherche des contraintes principales également utilisable en tectonique et en séismologie: la méthode des dièdres droits. *Bull. Soc. géol. Fr.* XIX, **6**, 1309–1318.

Armijo, R., Carey, E. & Cisternas, A. 1982. The inverse problem in microtectonics and the separation of tectonic phases. *Tectonophysics* **82**, 145–160.

Argus, D. F., Gordon, R. G., DeMets, Ch. & Stein, S. 1989. Closure of the Africa–Eurasia–North America plate motion circuit and tectonics of the Gloria Fault. *J. geophys. Res.* **94**, 5585–5602.

Asebriy, L., Bourgois, J., Cherkaoui, T.-E. & Azdimousa, A. 1993. Evolution tectonique récente de la zone de faille du Nékor: importance paléogéographique et structurale dans le Rif externe, Maroc. *J. Afr. Earth Sci.* **17**, 1, 65–74.

Bentaleb, B., Cherkaoui, T.-E., Herquel, G., Jebli, H. & Ramdani, F. 1984. Sismicité et evaluation du risque sismique dans le Maroc oriental. *Bull. Inst. Sci.*, **8**, 77–92.

Buforn, E. & Udias, A. 1991. Focal mechanism of earthquakes in the Gulf of Cadiz, south Spain and Alboran Sea. *Publ Instituto Geogr. Nacional, Madrid, Ser. Monografias* **8**, 29–40.

Buforn, E., Udias, A. & Colombas, M. A. 1988. Seismicity, source mechanisms and tectonics of the Azores–Gibraltar plate boundary. *Tectonophysics* **152**, 89–118.

Carey, E. 1979. Recherche des directions principales de contraintes associées au jeu d'une population de failles. *Rev. Géogr. phys. & Géol. dyn.* **21**, 57–66.

Carey, E. & Brunier, B. 1974. Analyse théorique et numérique d'un modèle mécanique élémentare appliqué à l'étude d'une population des failles. *C. r. Acad. Sci. Paris, sér. D* **279**, 397–400.

Carey-Gailhardis, E. & Mercier, J.-L. 1987. A numerical method for determining the state of stress using focal mechanisms of earthquake populations: application to Tibetan teleseisms amd microseismicity of Southern Peru. *Earth Planet. Sci. Lett.* **82**, 165–179.

Carey-Gailhardis, E. & Mercier, J. L. 1992. Regional state of stress, fault kinematics and adjustments of blocks in a fractured body of rock: application to the microseismicity of the Rhine graben. *J. Struct. Geol.* **14**, 1007–1017.

Cherkaoui, T.-E. 1988. Fichier des séismes du Maroc et des régions limitrophes 1901–1984. *Trav. Inst. Sci., sér. Géol. & géogr. phys.* **17**.

Cherkaoui, T.-E. 1991. Contribution à l'étude de l'aléa sismique au Maroc. University Thesis, Grenoble.

Cherkaoui, T.-E., Hatzfeld, D., Jebli, H., Medina, F. & Caillot, V. 1990. Etude microsismique de la région d'Al Hoceima. *Bull. Inst. Sci.* **14**, 25–34.

Chotin, P. & Aït Brahim, L. 1988. Transpression et magmatisme au Néogène-Quaternaire dans le Maroc oriental. *C. r. Acad. Sci. Paris, sér. II* **306**, 1479–1485.

Etchecopar, A., Vasseur, G. & Daignieres, M. 1981. An inverse problem in microtectonics for the determination of stress tensors from fault striation analysis. *J. Struct. Geol.* **3**, 1, 51–65.

Fraissinet, C. 1989. Les étapes de la structuration récente du Haut Atlas calcaire (Maroc). Analyse des rapports entre raccourcissement et surrection au sein d'une chaîne intracontinentale. University Thesis, Paris XI.

Frizon de Lamotte, D. 1982. Contribution à l'étude de l'évolution structurale du Rif oriental. *Notes & Mém. Serv. géol. Maroc.* **314**, 239–309.

Frogneux, M. 1980. La sismicité marocaine de 1972 à 1978. Etude des paramètres à la source des séismes proches. 3ème cycle Thesis, Grenoble.

Frohlich, C. & Apperson, K. D. 1992. Earthquake focal mechanisms, moment tensors, and the consistency of seismic activity near plate boundaries. *Tectonics* **11**, 279–296.

Galindo-Zaldivar, J., Gonzalez-Lodeiro, F. & Jabaloy, A. In press. Stress and palaeostress in the Betic–Rif cordilleras (Miocene to the present). *Tectonophysics* **227**.

Groupe de Recherche Néotectonique de l'Arc de Gibraltar 1977. L'histoire tectonique récente de l'Arc de Gibraltar. *Bull. Soc. géol. Fr.* XIX **3**, 591–605.

Guillemin, M. & Houzay, J. P. 1982. Le Néogène post-nappe et le Quaternaire du Rif nord-oriental. Stratigraphie et tectonique des bassins de Melilla, du Kert, de Boudinar et du piedmont des Kebdana. *Notes & Mém. Serv. géol. Maroc* **314**, 7–237.

Hatzfeld, D. 1978. Etude sismotectonique de la zone de collison ibéro-maghrébine. State Thesis, Grenoble.

Hatzfeld, D., Caillot, V., Cherkaoui, T.-E., Jebli, H. & Medina, F. 1993. Microearthquake seismicity and fault plane solutions study around the Nékor strike-slip fault, Morocco. *Earth Planet. Sci. Lett.* **120**, 31–41.

Hatzfeld, D., Christodoulou, A. A., Scordilis, E. M., Panagiotopoulos, D. & Hatzdimitriou, P. M. 1987. A microearthquake study of the Mygdonian graben (northern Greece). *Earth Planet. Sci. Lett.* **81**, 379–396.

Hatzfeld, D., Frogneux, M. & Girardin, D. 1977. Etude de la sismicité dans la région de l'arc de Gibraltar. *Bull. Soc. géol. Fr.* **4**, 741–747.

Hippolyte, J.-C., Angelier, J. & Roure, F. 1992. Les permutations d'axes des contraintes: exemples dans les terrains quaternaires du sud de l'Apennin (Italie). *C. r. Acad. Sci. Paris, sér. II*, **315**, 89–95.

Leblanc, D. & Olivier, P. 1984. Role of strike-slip faults in the Betic–Rifian orogeny. *Tectonophysics* **101**, 345–355.

Marrett, R. & Allmendinger, R. W. 1990. Kinematic analysis of fault slip data. *J. Struct. Geol.* **12**, 973–986.

Maurer, G. 1968. Les montagnes du Rif central: étude géomorphologique. Doctorat d'Etat Thesis, Paris.

McKenzie, D. P. 1969. The relation between fault plane solutions for earthquakes and the directions of the principal stresses. *Bull. seism. Soc. Am.* **59**, 591–601.

Medina, F. & Cherkaoui, T.-E. 1992. Mécanismes au foyer des séismes du Maroc et des régions voisines (1956–1986). Conséquences tectoniques. *Eclogae geol. Helv.* **85**, 433–457.

Minster, J. B. & Jordan, T. H. 1978. Present-day plate motions. *J. geophys. Res.* **83**, 5331–5354.

Moreira, V. S. 1985. Seismotectonics of Portugal and its adjacent area in the Atlantic. *Tectonophysics* **117**, 85–96.

Morel, J.-L. 1987. Evolution récente de l'orogène rifain et de son avant-pays depuis la fin de la mise en place des nappes (Rif, Maroc). *Mém. Géodiffusion, Orsay* **4**.

Morel, J.-L. 1992. Carte des mouvements récents du Rif au 1/500 000. *Notes & Mém. Serv. géol. Maroc* **365**.

Mourier, Th. 1982. Etude géologique et structurale de Massif des Bokkoya (Rif oriental, Maroc). 3ème cycle Thesis, Orsay.

Ouyed, M. 1981. Le tremblement de terre d'El Asnam du 10 octobre 1980. Etude des répliques. Thesis of 3ème cycle, Grenoble.

Philip, H. 1987. Plio-Quaternary evolution of the stress field in Mediterranean zones of subduction and collision. *Annales Geophys.* **5B**, 301–320.

Rebaï, S., Philip, H. & Taboada, A. 1992. Modern tectonic stress field in the Mediterranean region: evidence for variation in stress directions at different scales. *Geophys. J. Int.* **110**, 106–140.

Suter, G. 1980. Carte structurale de la chaîne rifaine au 1/500 000. *Notes & Mém. Serv. géol. Maroc* **245b**.

Thauvin, S. 1971. La zone rifaine. In: Serv. Géol. Maroc (edt) *Ressources en eau du Maroc*. Tome I: Domaines du Rif et du Maroc oriental. *Notes & Mém. Serv. géol. Maroc* **231**, 69–79.

Udias, A. & Buforn, E. 1991. Regional stresses along the Eurasia–Africa plate boundary derived from focal mechanisms of large earthquakes. *Pure & Appl. Geophys.* **136**, 433–448.

Udias, A., Lopez-Arroyo, A. & Mezcua, J. 1976. Seismotectonic of the Azores–Gibraltar region. *Tectonophysics* **31**, 259–289.

Zouine, E. M. 1993. Géodynamique récente du Haut Atlas. Evolution de sa bordure septentrionale et du Moyen-Atlas sud-occidental au cours du Cénozoïque. State Thesis, Rabat.